Urban heat island estimation from crowdsensing thermometers embedded in personal cars

Eva Marquès, Valéry Masson, Philippe Naveau, Olivier Mestre, Vincent Dubreuil, Yves Richard

BAMS Article

Urban Heat Island Estimation from Crowdsensing Thermometers Embedded in Personal Cars

Eva Marquès, Valéry Masson, Philippe Naveau, Olivier Mestre, Vincent Dubreuil, and Yves Richard

ABSTRACT: An ever-growing portion of the global population lives in urban areas. Cities are expanding quickly and consequently, the urban heat island effect has become a major health concern to maintain city dwellers' thermal comfort. For this reason, city planners want to access urban meteorological databases in local areas where specific attention is needed. With the growth of connected devices, it is possible to collect unusual but massive temperature measurements from people's activities. In this article, we study temperatures measured by thermometers embedded in everyday personal cars. To assess the quality of such opportunistic data, we first detect factors deteriorating the measurement. After preprocessing, the measurement error is then estimated thanks to two weather station networks providing a local-scale reference through the cities of Dijon and Rennes, France. The overall aggregation of private car temperature measurements allows us to estimate very precisely the urban heat island at a 200-m resolution. We detect the cooling effect of parks in Rennes and Paris urban areas. In Barcelona and Dijon, we observe the impact of regional environments and the orographic effect on the urban heat island. With our method, similar maps can be made accessible to every interested city in western Europe to target critical areas and support urban planning decisions.

KEYWORDS: In situ atmospheric observations; Heat islands; Urban meteorology; Data quality control; Temperature; Uncertainty

https://doi.org/10.1175/BAMS-D-21-0174.1
Corresponding author: Eva Marquès, E-mail: eva.marques@meteo.fr
In final form 10 January 2022

AFFILIATIONS: Marquès, Masson, and Mestre—Centre National de Recherches Météorologiques, Université de Toulouse, Météo-France, CNRS, Toulouse, France; **Naveau**—Laboratoire des Sciences du Climat et de l'Environnement, Paris, France; **Mestre**—Météo-France, Toulouse, France; **Dubreuil**—LETG-Rennes, UMR-6554-CNRS, Université de Rennes 2, Rennes, France; **Richard**—CRC-Biogéosciences, UMR-6282-CNRS, Université de Bourgogne-Franche-Comté, Dijon, France

* **ORCID: Marquès**—https://orcid.org/0000-0001-9817-6546; **Masson**—https://orcid.org/0000-0001-8807-0545; **Naveau**—https://orcid.org/0000-0002-7231-6210; **Dubreuil**—https://orcid.org/0000-0001-8383-805X

Currently more than half of the world's population lives in urban areas (Ritchie and Roser 2018), and this proportion will likely increase in decades to come. Perkins-Kirkpatrick and Lewis (2020) indicated that heat waves are becoming more intense and more frequent in the twenty-first century. This context is favorable to the urban heat island (UHI) effect, characterized by the difference between urban temperature and temperature of the surrounding countryside (Oke et al. 2017). Temperature is generally higher for urban than for rural areas, especially at night, which can have dramatic consequences on vulnerable people subject to heat stress. During the 2003 heat wave in Europe, Paris (France) UHI intensity and duration had an impact on elderly population mortality (Laaidi et al. 2012). In the West Midlands (England), around 50% of heat-related deaths during this event were also due to the UHI (Heaviside et al. 2016). In Shanghai (China), 30 years of meteorological records corroborated the impact of UHIs on heat-related mortality risk (Tan et al. 2010). In consequence, there is a clear need to produce more urban temperature maps to help governance and urban planners develop city mitigation strategies (Leal Filho et al. 2017; Parsaee et al. 2019).

Observation systems for the canopy layer urban heat island. This paper focuses on the canopy layer temperature defined in Oke et al. (2017) as the temperature of the air between surface and roof level. It corresponds to the layer where city dwellers live. Canopy layer temperature has a direct impact on people's thermal comfort. UHI can be observed at different horizontal scales: Oke et al. (2017) distinguished the micro-, local, and mesoscales. Microscale is the smallest scale, including the building or even the street (typical scale: between 10 m $\times$ 10 m and 20 m $\times$ 200 m), while local scale encompasses the entire block or the whole neighborhood (typical scale: between 0.5 km $\times$ 0.5 km and 2 km $\times$ 2 km). The mesoscale includes the whole city if not the entire urban area. In this study, we are interested in observing the three scales. At the street scale, the temperature field varies very locally due to multiple factors such as anthropogenic activities, 3D urban geometry, and air flows (Chudnovsky et al. 2004).

Urban air temperature in the canopy layer is mostly measured thanks to ground-based instruments settled around 1–2 m high. In urban environments, World Meteorological Organization criteria for weather station setup are difficult to meet. Even if Oke (2004) adapted them to properly collect downtown measurements, it is still challenging to set up weather stations in cities. Sites should be carefully selected in homogeneous and representative zones. Thermometers should ideally be protected from solar radiations and ventilated. It is also a challenge to deal with practical requirements specific to urban networks: finding a secured support for the equipment, acquiring official authorization for the setup, insuring data recovery and maintenance. Despite the urge to measure fine scale UHI, only a few cities have access

to dense thermometer networks. Many of them settle for measuring the difference between one rural and one urban site only, in other words they estimate the UHI *intensity*, also denoted *UHI magnitude*. Professional rural measurement frequently comes from the airport weather station, which is most of the time located in the outskirts of the city.

UHI is also measured through measurement campaigns. Muller et al. (2013) made a review of existing urban meteorological networks. As an example, Birmingham city has been equipped with a measurement network for a 20-month period (Bassett et al. 2016). Konstantinov et al. (2018) set up four networks in the northern polar region cities in the 2016/17 winter. In Spain, Acero et al. (2013) used both stationary and mobile devices during three measurement campaigns in the city of Bilbao. These short-lived campaigns rarely capture extreme events like heat waves. In some rare cases, urban weather station networks have been deployed and monitored for long-term research. In France, Toulouse (Dumas et al. 2021), Dijon (Richard et al. 2018, 2021), and Rennes (Dubreuil et al. 2011) cities have been equipped with tens of urban semiprofessional weather stations. Such recordings are essential to assess the quality of new types of data.

Crowdsourcing data for urban climate research. With the wide spread of connected devices, massive data are collected every day from the public. *Crowdsourcing* refers to all information collected by the people and made available for multiple applications. For mobile measurement devices, the term *crowdsensing* is used. We also distinguish *participatory* and *opportunistic* sensing depending on persons involvement in the data collection: they can actively record the data or simply be the vector of the measurement process. As evidenced by Muller et al. (2015), crowdsourcing data can be leveraged for climate and atmospheric sciences. Observations of this kind are logically abundant in highly frequented areas like cities. Meteorologists have begun to take advantage of this opportunistic data. For example, Overeem et al. (2013) investigated the potential of massive smartphone battery temperature data to map the UHI of eight international cities. They encountered the difficulty to measure real outdoor temperature since the human's body and its location affected recordings. Despite the use of a heat transfer model to recalculate air temperature from battery measurements, additional in-depth study would be necessary to achieve fine-scale reliable inference of urban temperatures. Droste et al. (2017) still managed to compare daily temperatures from different neighborhoods in São Paulo thanks to smartphone batteries. Other devices like citizen weather stations (CWS) have drawn the attention of climatologists. Meier et al. (2015), Fenner et al. (2017), and Chapman et al. (2017) demonstrated the high potential of CWS from Netatmo company to respectively examine Berlin's and London's UHI. However, due to the lack of shelter or inadequate CWS location, they found many erroneous observations in the collected data. Meier et al. (2017) suggested to elaborate a quality control, since then enriched by Varentsov et al. (2020) on Moscow and Feichtinger et al. (2020) on Vienna. Madelin and Dupuis (2019) developed another statistical method evaluated on Paris and Napoly et al. (2018) proposed a quality control process that can operate without any temperature reference in Berlin, Toulouse, or Paris. In previously cited case studies, the percentage of deleted observations ranged from 40% to 75% depending on the method. Recently, Venter et al. (2020) in Oslo and Zumwald et al. (2021) in Zurich used CWS to infer 2-m air temperature at very high spatial resolution with the help of satellite Earth observations, 30 m $\times$ 30 m and 10 m $\times$ 10 m, respectively. In Hammerberg et al. (2018), CWS were used to validate urban climate models in Vienna. To mutually improve the potential of each data source, De Vos et al. (2020) merged temperature data not only from CWS but from smartphone batteries as well. They also measured rainfall, solar radiation, wind, and air pressure with other opportunistic devices.

To enrich these existing diverse data sources, Mahoney and O'Sullivan (2013) suggested to explore the potential of connected vehicles data for atmospheric sciences. For road weather

applications, Anderson et al. (2012) ran an experiment to examine the observations of temperature and atmospheric pressure collected by nine vehicles. They recorded the data during various meteorological events in the winter season. For the air temperature, the magnitude of the error was close to 1°C. The National Center for Atmospheric Research (NCAR) initiated the Pikalert project (Siems-Anderson et al. 2019) to improve road weather forecasts with onboard connected devices. In the same vein, Germany's National Meteorological Service Deutscher Wetterdienst (DWD) and the car manufacturer Audi launched the FloWKar partnership detailed in Riede et al. (2019). Most recently, Bell et al. (2021) analyzed a 2-month trial dataset collected by a fleet of cars in late winter and early spring of 2018. They found that weather is likely to have an influence over onboard thermometers. In sunny weather conditions, the uncertainty was larger than during cloudy or rainy days. For urban climate research, Knight et al. (2010) involved participants to manually record the temperature displayed on their own cars to observe Manchester's UHI. To reduce measurement errors, they recommended to begin the recordings after several minutes of moving. Most recently, Météo-France has established a partnership with Continental, an automotive supplier, to evaluate the opportunity offered by private car thermometers for urban climate applications. Connected vehicles are now very common and traffic is dense in urban areas. Car data abundance is a tremendous added value for atmospheric sciences specialists who want to improve weather forecast models. In particular, car data assimilation has been recently explored in the pilot study of Siems-Anderson et al. (2020). But to make the best use of car thermometers, it is important to know how they behave in the urban environment, not only during the winter season but also in extremely hot conditions. As part of this initiative, a massive database of car measurements across western Europe has been recovered and is used in the following study.

Methodology for private car temperatures evaluation in urban climate purpose. In this paper, we evaluate the quality of opportunistic car temperatures for urban climate applications. To detect potential factors responsible for measurement errors, we first carried out a short experiment during the June 2019 heat wave. We show that car speed affects the measurement when solar radiation is intense. We then introduce a new massive dataset of private car thermometer measurements. Thanks to an exploratory analysis on this data, we confirm that solar radiation is a nuisance factor and provide a correction to handle it. The car temperature uncertainty is then estimated in comparison to two dense weather station networks initially dedicated to study the UHI of Rennes and Dijon French cities. To highlight the convenience of car thermometer data in urban climate research, we map UHIs in cities with different topographies at different times of the day. On Dijon and Rennes midsized cities, we compare the UHI obtained with cars to the one measured by the existing networks. We also give an overview of applications for the understanding of UHI behavior according to local and regional environment with two major cities: Paris and Barcelona.

Preliminary experiment with car thermometers

To complement the results of Anderson et al. (2012) and Bell et al. (2021) obtained in winter and spring seasons, we set up an experiment during the June 2019 heat wave in Toulouse. We wanted to test the influence of the car's speed on the measured temperature under intense solar radiation and in an urban environment. The private car thermometer is generally embedded under the right-side mirror (or inside the front bumper) to minimize the effect of solar radiation. However, it measures the outdoor temperature with a low-cost sensor surrounded by a black material. In our experiment, a setup provided by Continental company collected temperatures from a single driving car. Air temperature was also measured by a static semiprofessional weather station. The car followed a short circuit with different speeds. Figure 1 shows that when the car stopped, temperature recorded by the car sensor can be up to 7°C higher than the reference weather station

protected from solar radiation. The gap decreases after departure during approximately 10 min and increases slowly during 15 min when the car stopped again. This is explained by the fact that the faster a car goes, the more its sensor is ventilated. When sun exposure is intense, measurement error decreases with speed after several minutes of travel, since ventilation takes effect. In high solar radiation conditions, it is reasonable to drop automatically all data whose speed is below a given threshold (we empirically settle it to 10 km h^{-1}).

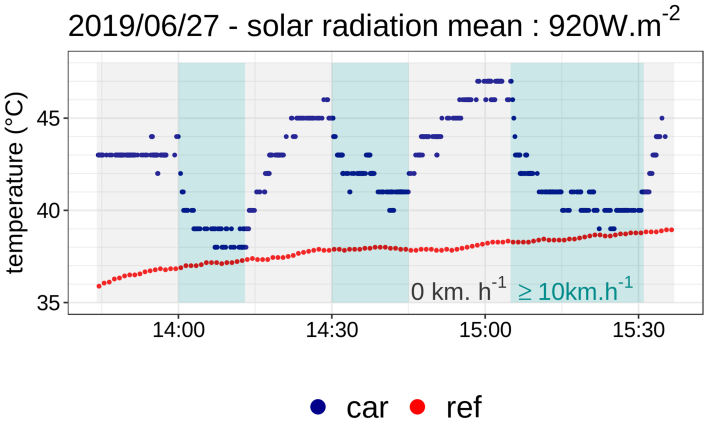

Fig. 1. Impact of speed on car temperature from 27 Jun 2019 measurement campaign of a driving car during heat wave. Gray areas: car is stopped. Blue areas: car's speed is greater than or equal to 10 km h^{-1}. Red points: reference temperature from a fixed weather station. Blue points: car's temperatures.

Estimation of car thermometer error with a massive database

PSA air temperature database. We retrieve a large dataset of 6.7 billion temperature recordings (700 GB) collected by cars of the brand Peugeot Société Anonyme (PSA) from June 2016 to December 2018. The PSA car manufacturer collects information from connected vehicles via a specific insurance contract purchased by some of their clients. In doing so, the clients consent to send personal data from their connected vehicles to the company in return for specific insurance services. In the dataset, each observation is a pointwise record of temperature packed with some metadata: GPS coordinates, timestamp accurate to the second, vehicle speed rounded to 5 km h^{-1}, and altitude. The thermometer records one temperature per minute rounded to the nearest 0.5°C.

For privacy policy reasons, car tracking is not allowed so the ID for each travel is not provided. As a consequence, the data are not supplied in a time series format but rather in the form of unrelated single observations. It is impossible to know if two measurements originate from the same car. We cannot enumerate the cars involved in available recordings but we notice that the amount of observations quickly increases in time, probably due to the growth of connected vehicles on the road. As a matter of fact, 24 million measurements were collected in June 2016 against 623 million 2 years later in June 2018.

PSA cars are mainly deployed in western Europe, so the dataset covers not only French metropolitan territory but also other European areas, especially Spain, Portugal, England, and Benelux (Fig. 2). Geographical and temporal distributions are directly related to road traffic intensity (Fig. 3). There is a clear contrast between diurnal and nocturnal periods. By night, while the UHI generally reaches its peak, observations are less abundant (Fig. 4). Roads are also highly frequented during rush hours and less busy on weekends.

We want to test if this database is exploitable even if we do not have all information about the sensor position on each car, its age and its behavior in a road and urban environment. In the following section, PSA car data are compared to the measurements of two weather station networks in the cities of Dijon and Rennes.

Reference temperature description: Dijon and Rennes dense weather station networks. Dijon and Rennes are two midsized French cities (respectively around 385,000 and 740,000 inhabitants for the whole urban area) with still operating weather station networks (Table 1). Both networks were initially used to measure air temperature and compute the UHI. The network

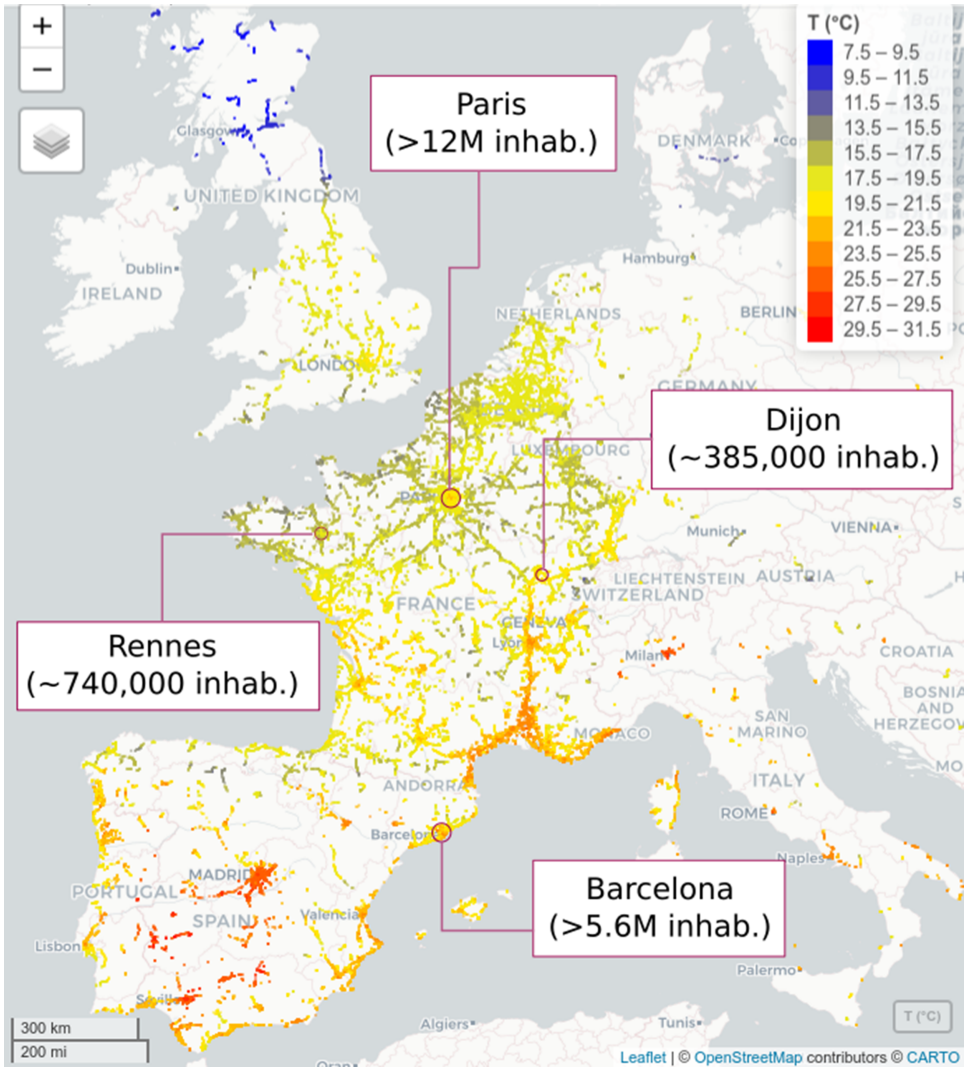

Fig. 2. A 1-h snapshot of private car observations from a database provided by PSA company (2100 UTC 19 Jun 2018). The temperature is measured with onboard thermometers across Europe. Dijon and Rennes midsized cities are used to estimate car data uncertainty and urban climate applications are tested on Paris and Barcelona megapolis. Urban areas population figures are from the UN Department of Economic and Social Affairs (2018) website.

Measuring Urban Systems Temperature of Air Round Dijon (MUSTARDijon) was deployed in 2014 (Pohl et al. 2015). In Rennes, numerous weather stations were installed since 2004 (Dubreuil et al. 2011) as part of the project Ecologie du rural vers l'urbain (ECORURB). Specification of the chosen thermometers indicates an accuracy better than 0.3°C. A methodological attention was paid to choose the location of weather stations. Most of the local climate zones described in Stewart and Oke (2012) classification were identified in both cities. Then, they equipped the corresponding representative areas with a weather station so that the diversity of urban environments was well represented (Richard et al. 2018). Weather stations were positioned in nonshaded zones, under meteorological shelters to protect the sensors from solar radiation. Also, a minimum distance of 2 m was kept between

Table 1. Dijon and Rennes weather station networks specifications.

Agglomeration	Project	Period	No. of stations	Weather station model	Accuracy	Resolution
Dijon	MUSTARDijon	2014–present	52	HOBO Pro V2	±0.21°C	0.02°C
Rennes	ECORURB	2004–present	22	Davis Weather Monitor II and Vantage Pro 2	±0.3°C	0.1°C

stations and surrounding urban elements such as walls or trees. For safety reasons, they were generally fixed on candelabra around 3 m high.

Method for car temperature uncertainty estimation. To estimate car temperature error ΔT, we select all car observations located within 200 m to at least one weather station from the reference network. This distance is at the limit between micro- and local scale. For this sample, ΔT_i is equal to the difference between the ith car measurement T_i and the temperature of the nearest reference station $T_{\mathrm{ref},i}$:

$$\Delta T_i = T_i - T_{\mathrm{ref},i}. \tag{1}$$

The study is performed in June–August 2018 because, in the summertime, atmospheric conditions are more likely favorable to intense UHIs, especially when solar radiation is intense and wind speed is low. According to the previous findings on the impact of vehicle speed, all observations under 10 km h^{-1} are removed. Due to car traffic variations, observations are not equally distributed in time. Frequencies are especially low by night. Nevertheless, for both cities the lowest frequency is achieved at 0100 UTC, and at this schedule, 174 observations are available in Dijon and 91 in Rennes.

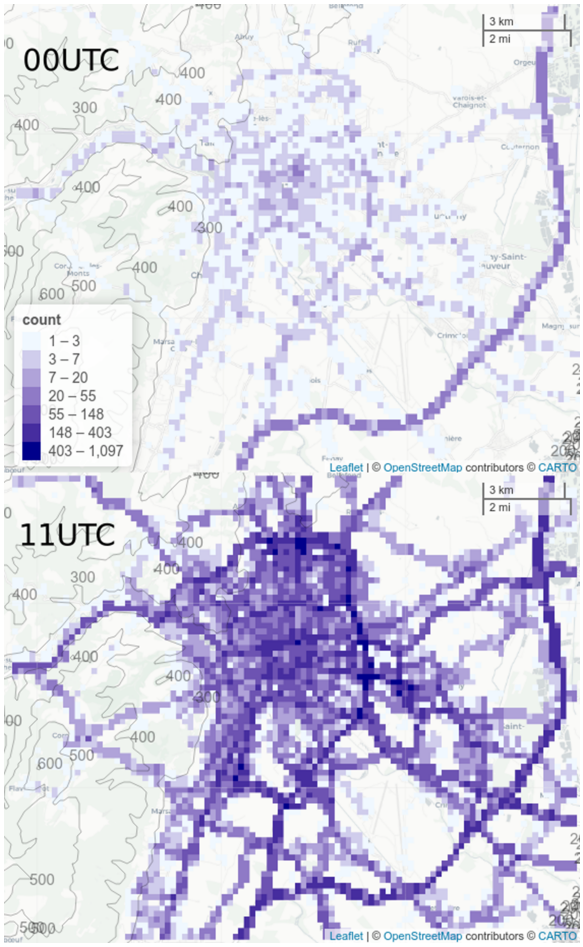

Fig. 3. Sum on a 200 m × 200 m resolution grid of all private car observations recorded during the 2018 summer at (top) 0000 and (bottom) 1100 UTC on Dijon agglomeration (logarithmic color scale).

Correction according to incoming solar radiation. To check the effect of sun exposure on measurement, we plot the anomaly ΔT defined in (1) according to incoming solar radiation intensity (Fig. 5). We neglect the effect of shadows along the vehicle travel and consider that incoming solar radiation is uniform across the spatial domain. The anomaly ΔT increases with shortwave radiation. In consequence, we build a linear regression model between the incoming solar radiation (explanatory variable)

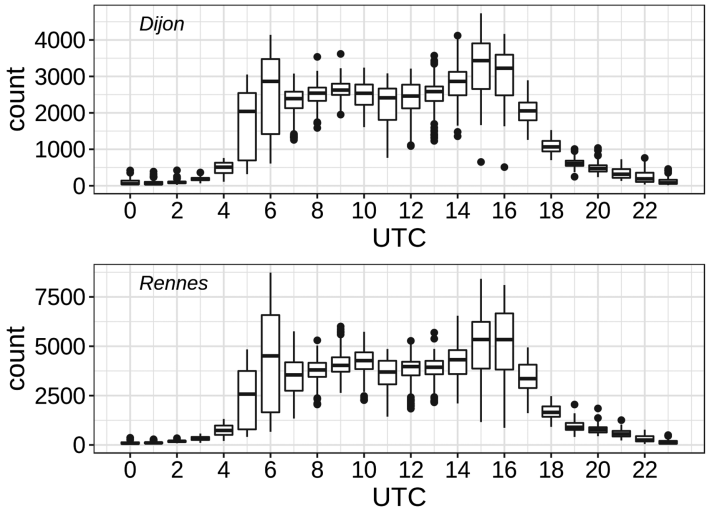

Fig. 4. Boxplots of the number of private car observations recorded hourly in the Dijon and Rennes French cities during the 2018 summer.

and the temperature anomaly ΔT (response variable):

$$\Delta T = \alpha + \beta \mathrm{SW} + \varepsilon. \qquad (2)$$

SW is the incoming solar radiation (W m^{-2}) measured by the Météo-France pyranometer (respectively located at Longevic airport for Dijon and St-Jacques airport for Rennes) and ε is the linear regression error. The α and β coefficients are estimated for both cities with summer diurnal observations in the neighborhood of reference weather stations. The ordinary least squares estimation gives $\hat{\alpha} = 0.3949$ for Rennes, $\hat{\alpha} = 0.2466$ for Dijon, $\hat{\beta} = 0.0025$ for Rennes, and $\hat{\beta} = 0.0034$ for Dijon. We then compute T_{corr} the corrected temperature

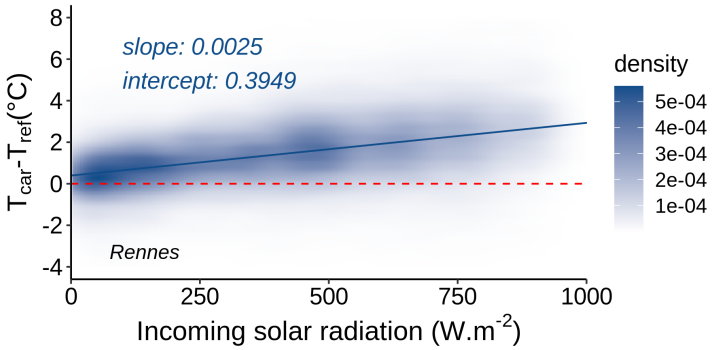

Fig. 5. Density plot of the difference between diurnal car observation and reference temperature (reference weather station located within 200 m) according to incoming solar radiation in Rennes in the 2018 summer.

$$T_{corr} = T_{raw} - \widehat{\Delta T} \qquad (3)$$

where $\widehat{\Delta T}$ is the ΔT (°C) predicted with regression model (2) and T_{raw} is the initial temperature (°C). Solar radiation correction is applied to avoid overestimation of diurnal temperatures. At each time step, the correction is the same across the spatial domain. For intense solar radiation (900 W m^{-2}), corrections applied in Rennes and Dijon are respectively $T_{raw} - 2.65$°C and $T_{raw} - 3.30$°C. Further analysis should be run to understand the difference between both cities and suggest a generalized correction for other cities.

Car sensor–estimated specifications. After solar radiation correction, 70% of observations have an absolute difference $|\Delta T|$ under 1°C in nighttime and under 1.4°C during the day (Fig. 6). We obtain asymptotic 95% confidence intervals for the mean μ and the uncertainty σ of the difference $\widehat{\Delta T}$ (Table 2). The estimated mean is close to zero for both cities, daytime as well as at night. The standard deviation σ is around 1.5°C for Dijon and 1.6°C for Rennes but varies significantly depending on the solar radiation intensity. It is approximately 0.45°C lower for nocturnal observation and 0.40°C higher when incoming solar radiation is intense. The interquartile range also varies in the day (Fig. 7): it increases until 1100 UTC at the

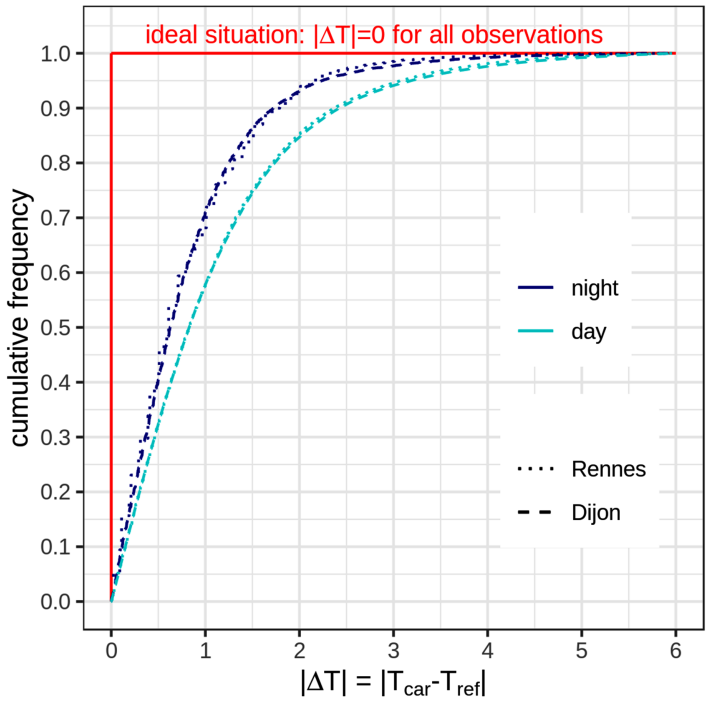

Fig. 6. Estimated cumulative density of the diurnal and nocturnal absolute error for Dijon and Rennes in the 2018 summer. By night, a larger portion of observations has an absolute error inferior to 1°C. The ideal case is when car temperature is equal to reference temperature for all observations.

Table 2. Asymptotic 95% confidence intervals for the mean μ and standard deviation σ of $\widehat{\Delta T}$ for both cities.

City	Incoming solar radiation	n	$CI_{95\%}(\mu)$	$CI_{95\%}(\sigma)$
Dijon	[0, 1,000] W m^{-2} (all the observations)	178,103	[−0.02, −0.01]	[1.60, 1.62]
Rennes	[0, 1,000] W m^{-2} (all the observations)	44,146	[−0.00, 0.02]	[1.48, 1.52]
Dijon	0 W m^{-2} (night)	10,880	[−0.15, −0.11]	[1.11, 1.19]
Rennes	0 W m^{-2} (night)	2,919	[−0.35, −0.28]	[1.00, 1.11]
Dijon	≥700 W m^{-2} (high solar radiation)	40,317	[−0.04, 0.00]	[2.04, 2.08]
Rennes	≥700 W m^{-2} (high solar radiation)	6,910	[−0.13, −0.05]	[1.86, 1.96]

zenith and decreases then, which seems to confirm that the variability is correlated to the solar radiation. However, it can also be a consequence of the choice to take a 200-m radius to select the observed sample: the microscale variability is not taken into account.

Urban heat island observation with car sensors

Adequacy of car thermometers for urban heat island observation. Car thermometers constitute a new way to measure UHIs. Stewart (2011) depicts rigorous practices to adopt when publishing on the canopy layer UHI. To assess car temperatures' usefulness for urban climate research, we discuss their characteristics in regard to the five requirements directly related to the measurement device (Table 3). In particular, car thermometer specifications estimated in the previous section meet the criterion (3), which imposes to indicate these specifications for each measurement device. Criteria (4) and (6) on site measurement metadata and on the number of observations, respectively, mainly designed for fixed weather stations, can still be fulfilled in studies based on crowdsensing data like car temperatures.

We compute the UHI on several cities for summer 2018. For each hourly time step t, the UHI temperature at the s location is the difference between car measurement and a temperature baseline:

$$T_{\mathrm{UHI}}(s,t) = T_{\mathrm{car}}(s,t) - T_{\mathrm{baseline}}(t). \tag{4}$$

In the literature, the baseline temperature is generally measured by a fixed weather station chosen in a representative rural environment near the city. However, car observations are not emitted from fixed locations and we cannot determine a rural reference visited at each time step. For this reason, we define the baseline temperature as the first decile of all car observations. Our method is applicable to any city, no matter its topography. The temperature differences between neighborhoods are not impacted by the strategy chosen to fix the baseline. The UHI value at one location has to be interpreted in regard to the areas where the UHI is null. In the following maps, the baseline temperature corresponds to gray grid points, mainly located in rural areas around the cities.

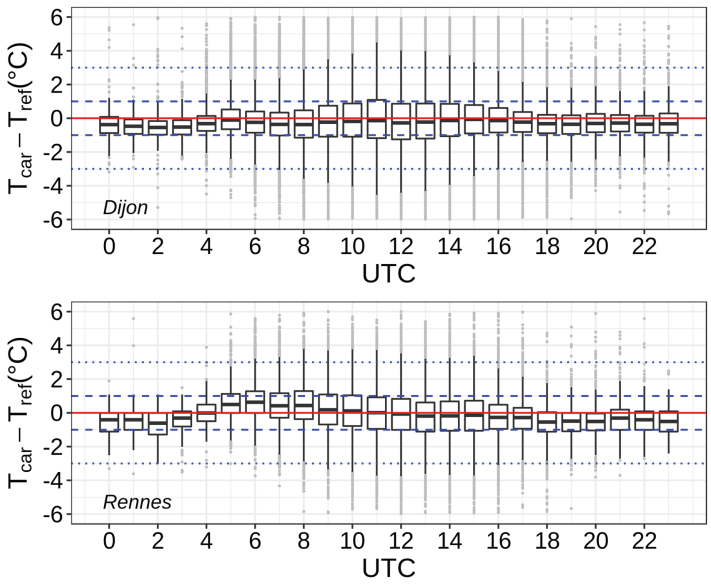

Fig. 7. Boxplots of the hourly difference between car observation and the nearest reference weather station (located within 200 m) for Dijon and Rennes in the 2018 summer.

Table 3. Car thermometer data with regard to Stewart (2011; numbers in parentheses in the first column) criteria related to measurement device for urban canopy UHI study.

	Requirement	Car thermometers adequacy
(3)	Measurement device specifications mentioned	Official specifications are not delivered. We estimate the error mean $\mu \approx 0°C$ and standard deviation $\sigma \approx 1.55°C$.
(4)	Site measurement metadata and microscale description	Cars GPS coordinates are precise to 5–10 m. Cars temperatures are logically measured above mineral soil.
(6)	Number of observations and replicates	Frequency depends on road traffic and varies in time and space.
(9)	Measurement synchronicity	Cars timestamp resolution is to the second.

Before drawing maps, we discard observations from low-speed vehicles. To counteract the unwanted influence of elevation on UHI computation, we add an altitude correction of 0.6°C every 100 m (Stewart 2011). All observations in tunnels have to be removed since they are not representative of air temperature in the canopy layer. We do not apply the solar radiation correction depicted in the section "Correction according to incoming solar radiation" because we map the UHI intensity and not the temperature: T_{baseline} and T_{car} are both measured by cars at the same time step and the correction is the same on the whole spatial domain. This way, UHI maps can be drawn for any city.

Aggregation method for mapping crowdsensing data. One particularity of crowdsourcing observations is that the data user is not involved in the measurement process. The location and time of measurement are not under control and, especially with mobile recordings, observations are sparse and randomized. In return, we can take advantage of the observation abundance and compute the local tendency thanks to a spatiotemporal aggregation. We aggregate the data per hour on a 200-m resolution grid and compute for each grid point the median of the car observations. The grid points with fewer than 15 observations are deleted in order to have a minimum sample size for median estimation. Then, at each grid point we average the UHI obtained at the same moment of the day for all 2018 summer. A 95% confidence interval can be computed for each local median and the map of its range gives an indicator about the uncertainty of the local tendency (Fig. 8).

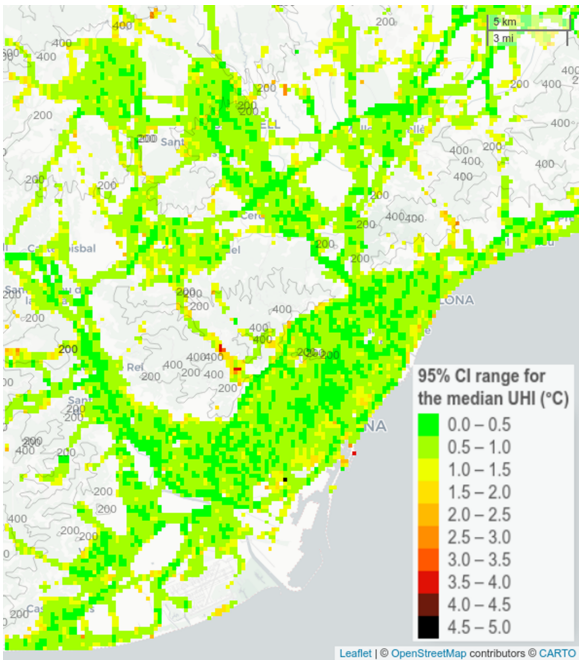

Fig. 8. Map of the range of the 95% confidence interval for the estimated median UHI (1800 UTC summer 2018) at each 200 m × 200 m grid point for Barcelona agglomeration. All grid points with less than $n = 15$ observations are removed. Orographic isolines indicate 200-m drops.

UHI maps and discussion on diverse European cities. Car data quantity is sufficient across medium-sized cities to map the UHI. For example, the median UHI inferred in Dijon and Rennes by car thermometers recordings during the 2018 summer is mapped in Figs. 9 and 10. It is very close to the one recorded by semiprofessional weather stations. In addition to MUSTARDijon and ECORURB networks, private car data expand the spatial coverage and provide fine-scale information not yet available until now on these cities.

Dijon is subject to both diurnal and nocturnal UHIs (Fig. 9). By night, the historical center is up to 5°C higher than the

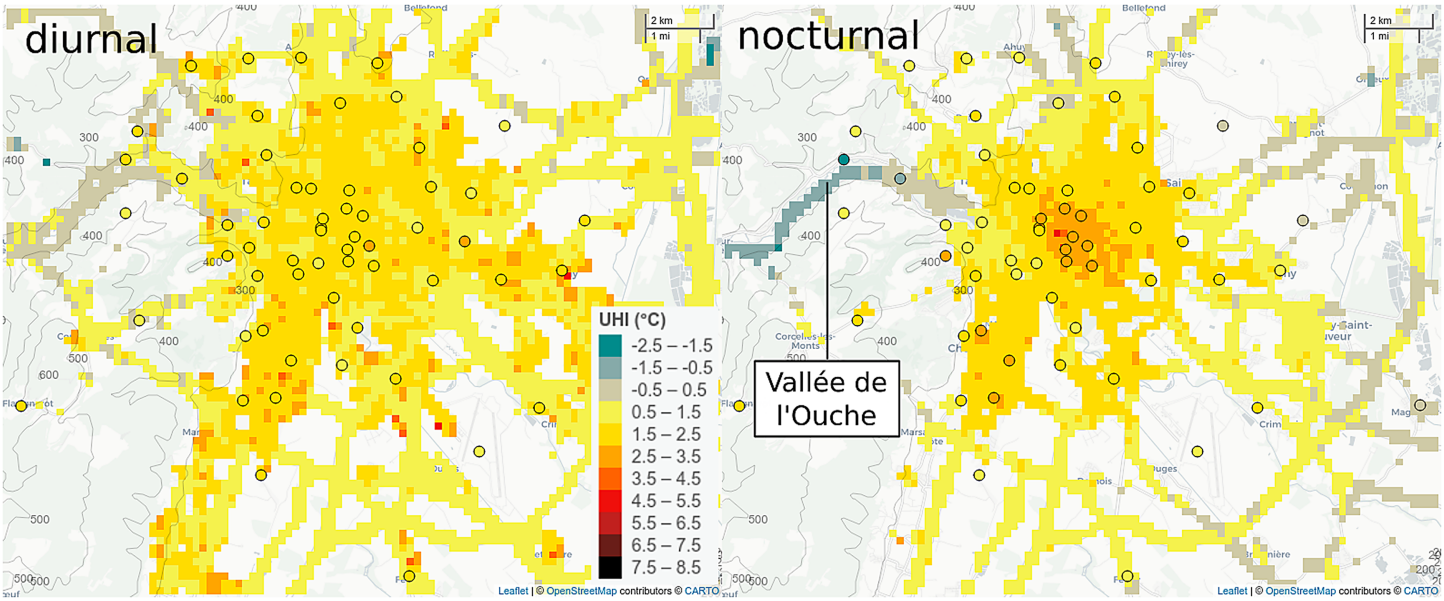

Fig. 9. (left) Diurnal and (right) nocturnal median UHI from personal car onboard thermometers in Dijon during the 2018 summer (200 m × 200 m resolution grid). Observations from low-speed vehicles are removed. Temperature vertical gradient due to topography is corrected (0.6°C added every 100 m). The UHI temperature baseline (gray areas) is given by the 1st-decile temperature of all observations. Circles: temperatures measured by MUSTARDijon semiprofessional network. Orographic isolines indicates 100-m drops.

temperature of the plain in the east. To the west, after correction of the altitude gradient, we observe a thermal inversion of 3°C between 250- and 400-m altitude. We suppose that a katabatic wind flows down from the plateau (600-m altitude) and cools the Ouche Valley.

In Rennes (Fig. 10), the nocturnal UHI is shifted to the south of the city, which is coherent with the observation of Dubreuil et al. (2020). It could partly be explained by the presence

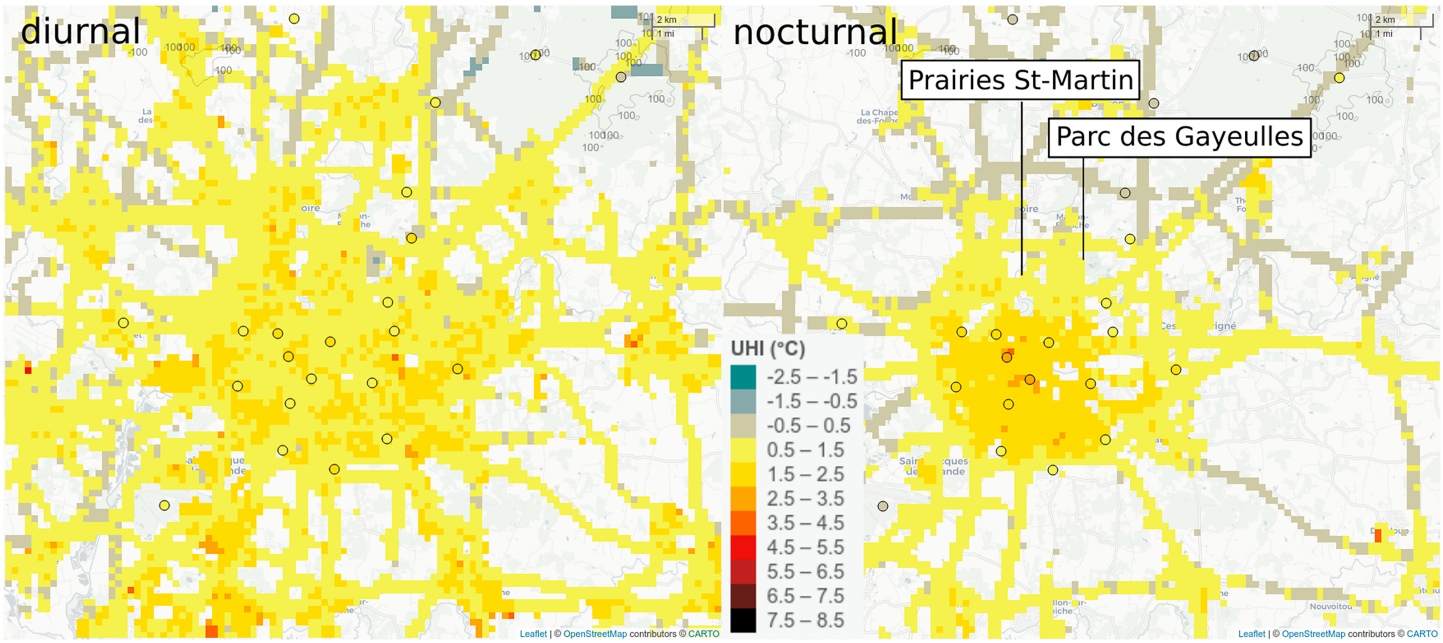

Fig. 10. (left) Diurnal and (right) nocturnal median UHI from personal car onboard thermometers in Rennes during the 2018 summer (200 m × 200 m resolution grid). Observations from low-speed vehicles are removed. Temperature vertical gradient due to topography is corrected (0.6°C added every 100 m). The UHI temperature baseline (gray areas) is given by the 1st-decile temperature of all observations. Circles: temperatures measured by ECORURB semiprofessional network. Orographic isolines indicates 100-m drops.

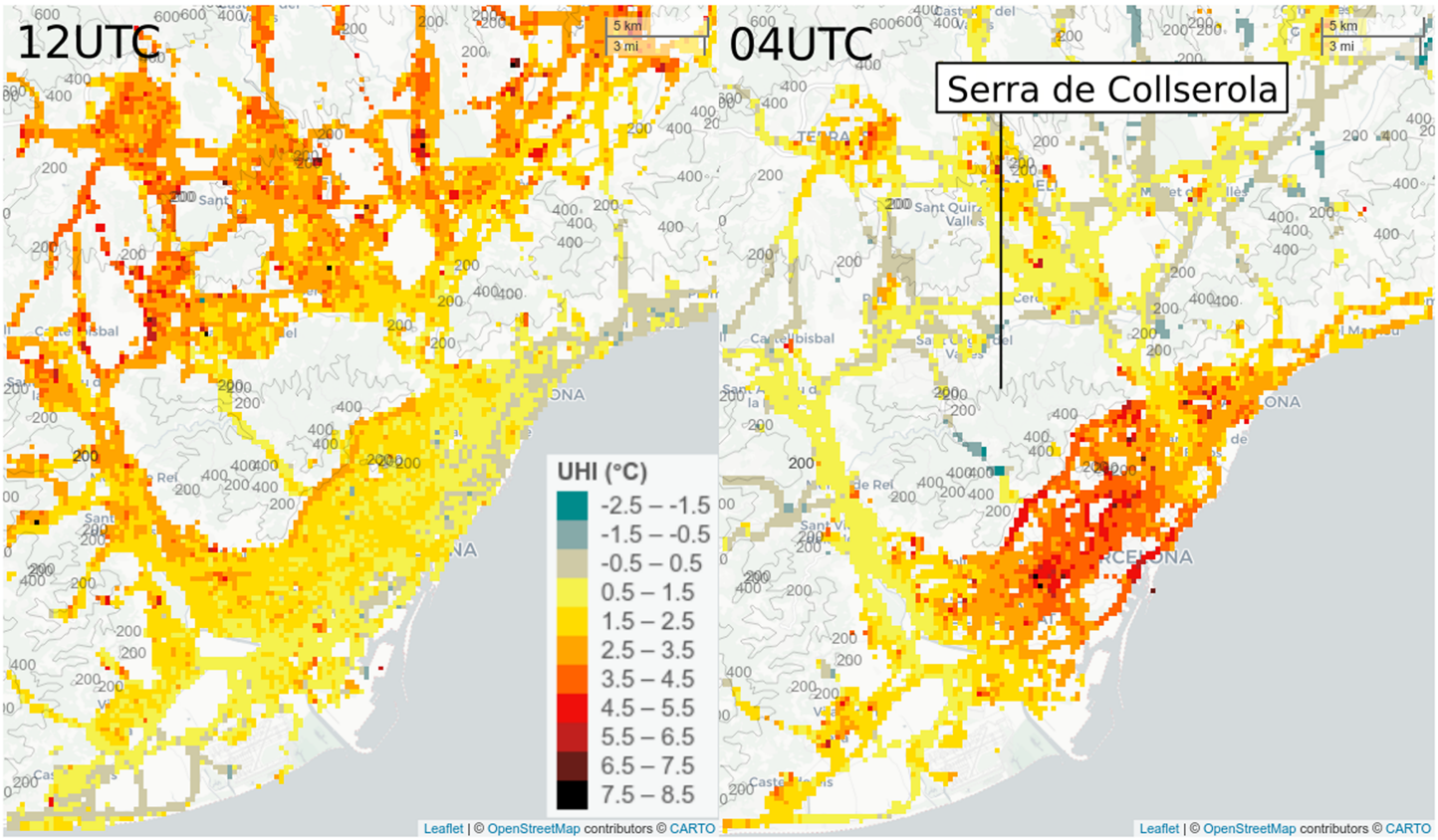

Fig. 11. Hourly median UHI at (left) 1200 and (right) 0400 UTC from personal car onboard thermometers in Barcelona during the 2018 summer (200 m × 200 m resolution grid). Observations from low-speed vehicles are removed. Temperature vertical gradient due to topography is corrected (0.6°C added every 100 m). The UHI temperature baseline (gray areas) is given by the 1st-decile temperature of all observations. Orographic isolines indicates 200-m drops.

of wooded parks in the northeastern part of the city. A few kilometers to the northeast, the wide forest is cooler than the surrounding countryside.

The density of personal cars within large cities located in complex geographical terrains allows us to make assumptions on interactions between urban climate and other meteorological phenomena. For example, the coastal megapolis of Barcelona (Spain) dominated on the northwest by the massif of Serra de Collserola is subject to both meteorological and orographic features (Fig. 11). In accordance with Salvati et al. (2017), diurnal temperatures are higher behind the Serra de Collserola than in the historical center located near the coast and cooled by the sea breeze. The warmest urban areas are suburbs located a few kilometers inland. A similar configuration was previously observed by a weather station network in the plain downwind of Tokyo metropolis (Yamato et al. 2017). In contrast, at night the sea breeze disappears and the warmest zones migrate near the coastal line, in the extremely dense historical center. The Serra de Collserola hill does not seem to produce a significant cooling effect through katabatic flow. The quantification of the relative intensities of both urban and orographic phenomena would require further analysis.

Private car data can be efficiently leveraged to get information on fine spatial features. We can distinguish the warmest and coolest neighborhoods in Paris during the July 2018 heat wave (Fig. 12). For example on the map, La Défense financial district is 4°–5°C higher than the residential area located a few kilometers on the west. Also, even if parks and forests are rarely crossed by cars, we still observe that Bois de Boulogne and Buttes-Chaumont parks are 1°–3°C cooler than the rest of Paris center. Nevertheless, the Bois de Vincennes is not enough explored to conclude its cooling effect. To the northwest, the forest of St-Germain-en-Laye is particularly cold.

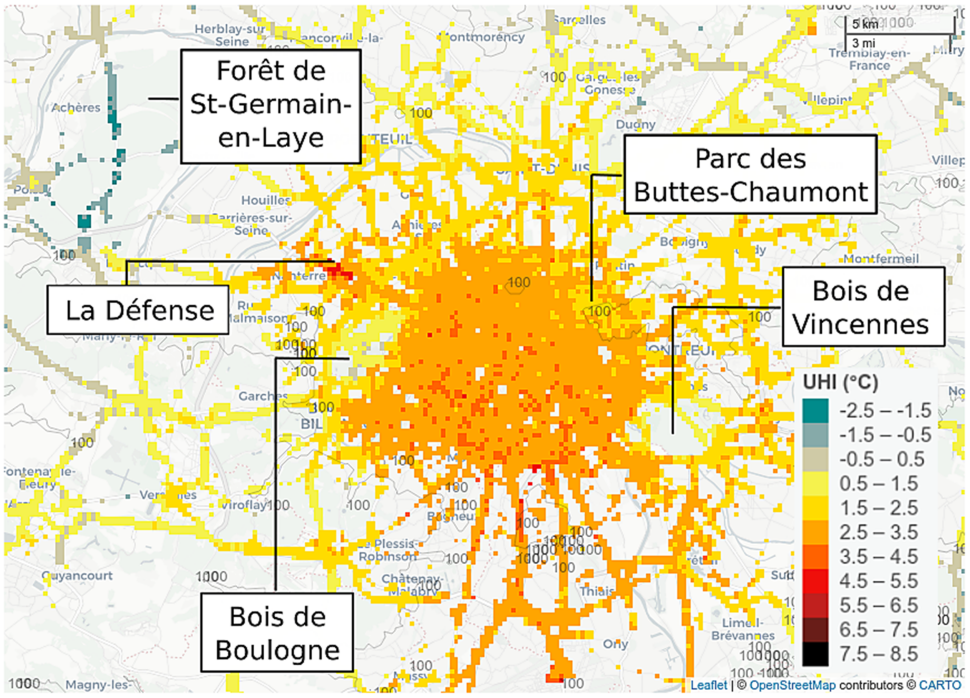

Fig. 12. Nocturnal median UHI (1–9 Aug 2018) in Paris during the 2018 heat wave (200 m × 200 m resolution). Observations from both low-speed vehicles and cars in tunnels are removed. Temperature vertical gradient due to topography is corrected (0.6°C added every 100 m). The UHI temperature baseline (gray areas) is given by the 1st-decile temperature of all observations. La Défense is the financial district of Paris. Orographic isolines indicate 100-m drops.

Conclusions

In response to current limitations to expand traditional observation systems in urban areas, private car thermometers considerably increase the density of air temperature observations. Similarly to all crowdsourced data previously studied for UHI study, particular attention is needed concerning the quality evaluation. After the removal of low speeds and a linear correction of solar radiation effect, the estimated mean error is close to zero during both day and night. At night, uncertainty is low ($\sigma \approx 1.1$°C) but observations are generally too sparse. To address this issue, data from other sources could be added to car temperatures. For example, the database can be completed with existing professional networks or CWS such as Netatmo network. Highly trusted sources could potentially be used as calibration references to correct those which are more uncertain. During the day, car data are voluminous but uncertainty is higher than by night ($\sigma \approx 2$°C). It can probably be explained by microscale variations of temperature occurring during the daytime.

The large amount of car data allows us to precisely estimate fine-scale UHIs in many cities with a 200 m × 200 m aggregation. As shown for Dijon, Rennes, Paris, and Barcelona it represents a huge potential to carry on urban climate research. Also, medium-sized cities hosting hundreds of thousands of inhabitants can now have access to local-scale UHI observation. We can also study very specific events like heat waves or focus on one special night. With the help of complex statistical models in future work, we could take into account urban morphology indicators provided in databases such as MApUCE data collected as part of the project Modélisation Appliquée et droit de l'Urbanisme: Climat urbain et Énergie (Bocher et al. 2018). Also, beyond urban climate interests, connected vehicles provide a huge amount of observations that would likely interest other meteorological specialists for verification or data assimilation in weather forecast models.

Acknowledgments. Private car database acquisition has been possible thanks to the supervision of Yann Guillou (Météo-France) as an intermediary with PSA company. The setup that collects the data

from the car thermometer during the measurement campaign has been provided as part of the partnership with Continental company. Nadine Aniort has played a key role by managing the project at Météo-France. We would finally like to cite the powerful language we mainly use: R Core Team (2019), thanks to which all this work has been done.

Data availability statement. Car data samples can be made available for research purpose by means of a partnership with Météo-France. For MUSTARDijon and ECORURB data, please do not hesitate to address the referents, respectively Yves Richard and Vincent Dubreuil.

References

Acero, J. A., J. Arrizabalaga, S. Kupski, and L. Katzschner, 2013: Urban heat island in a coastal urban area in northern Spain. *Theor. Appl. Climatol.*, **113**, 137–154, https://doi.org/10.1007/s00704-012-0774-z.

Anderson, A. R. S., M. Chapman, S. D. Drobot, A. Tadesse, B. Lambi, G. Wiener, and P. Pisano, 2012: Quality of mobile air temperature and atmospheric pressure observations from the 2010 development test environment experiment. *J. Appl. Meteor. Climatol.*, **51**, 691–701, https://doi.org/10.1175/JAMC-D-11-0126.1.

Bassett, R., X. Cai, L. Chapman, C. Heaviside, J. E. Thornes, C. L. Muller, D. T. Young, and E. L. Warren, 2016: Observations of urban heat island advection from a high-density monitoring network. *Quart. J. Roy. Meteor. Soc.*, **142**, 2434–2441, https://doi.org/10.1002/qj.2836.

Bell, Z., S. L. Dance, and J. A. Waller, 2021: Exploring the characteristics of a vehicle-based temperature dataset for convection-permitting numerical weather prediction. arXiv, 28 pp., https://doi.org/10.48550/arXiv.2105.12526.

Bocher, E., G. Petit, J. Bernard, and S. Palominos, 2018: A geoprocessing framework to compute urban indicators: The MApUCE tools chain. *Urban Climate*, **24**, 153–174, https://doi.org/10.1016/j.uclim.2018.01.008.

Chapman, L., C. Bell, and S. Bell, 2017: Can the crowdsourcing data paradigm take atmospheric science to a new level? A case study of the urban heat island of London quantified using Netatmo weather stations. *Int. J. Climatol.*, **37**, 3597–3605, https://doi.org/10.1002/joc.4940.

Chudnovsky, A., E. Ben-Dor, and H. Saaroni, 2004: Diurnal thermal behavior of selected urban objects using remote sensing measurements. *Energy Build.*, **36**, 1063–1074, https://doi.org/10.1016/j.enbuild.2004.01.052.

De Vos, L., A. Droste, M. Zander, A. Overeem, H. Leijnse, B. Heusinkveld, G. Steeneveld, and R. Uijlenhoet, 2020: Hydrometeorological monitoring using opportunistic sensing networks in the Amsterdam metropolitan area. *Bull. Amer. Meteor. Soc.*, **101**, E167–E185, https://doi.org/10.1175/BAMS-D-19-0091.1.

Droste, A., J.-J. Pape, A. Overeem, H. Leijnse, G.-J. Steeneveld, A. Van Delden, and R. Uijlenhoet, 2017: Crowdsourcing urban air temperatures through smartphone battery temperatures in São Paulo, Brazil. *J. Atmos. Oceanic Technol.*, **34**, 1853–1866, https://doi.org/10.1175/JTECH-D-16-0150.1.

Dubreuil, V., H. Quénol, X. Foissard, and O. Planchon, 2011: Climatologie urbaine et îlot de chaleur urbain à Rennes. *Ville et biodiversité: les enseignements d'une recherche pluridisciplinaire*, P. Clergeau, Ed., Presses Universitaires de Rennes, 105–122.

——, X. Foissard, J. Nabucet, A. Thomas, and H. Quénol, 2020: Fréquence et intensité des îlots de chaleur à Rennes: bilan de 16 années d'observations (2004–2019). *Climatologie*, **17**, 6, https://doi.org/10.1051/climat/202017006.

Dumas, G., V. Masson, J. Hidalgo, V. Edouart, A. Hanna, and G. Poujol, 2021: Co-construction of climate services based on a weather stations network: Application in Toulouse agglomeration local authority. *Climate Serv.*, **24**, 100274, https://doi.org/10.1016/j.cliser.2021.100274.

Feichtinger, M., R. de Wit, G. Goldenits, T. Kolejka, B. Hollósi, M. Žuvela Aloise, and J. Feigl, 2020: Case-study of neighborhood-scale summertime urban air temperature for the city of Vienna using crowd-sourced data. *Urban Climate*, **32**, 100597, https://doi.org/10.1016/j.uclim.2020.100597.

Fenner, D., F. Meier, B. Bechtel, M. Otto, and D. Scherer, 2017: Intra and inter local climate zone variability of air temperature as observed by crowdsourced citizen weather stations in Berlin, Germany. *Meteor. Z.*, **26**, 525–547, https://doi.org/10.1127/metz/2017/0861.

Hammerberg, K., O. Brousse, A. Martilli, and A. Mahdavi, 2018: Implications of employing detailed urban canopy parameters for mesoscale climate modelling: A comparison between WUDAPT and GIS databases over Vienna, Austria. *Int. J. Climatol.*, **38**, e1241–e1257, https://doi.org/10.1002/joc.5447.

Heaviside, C., S. Vardoulakis, and X.-M. Cai, 2016: Attribution of mortality to the urban heat island during heatwaves in the West Midlands, UK. *Environ. Health*, **15**, S27, https://doi.org/10.1186/s12940-016-0100-9.

Knight, S., C. Smith, and M. Roberts, 2010: Mapping Manchester's urban heat island. *Weather*, **65**, 188–193, https://doi.org/10.1002/wea.542.

Konstantinov, P., M. Varentsov, and I. Esau, 2018: A high density urban temperature network deployed in several cities of Eurasian Arctic. *Environ. Res. Lett.*, **13**, 075007, https://doi.org/10.1088/1748-9326/aacb84.

Laaidi, K., A. Zeghnoun, B. Dousset, P. Bretin, S. Vandentorren, E. Giraudet, and P. Beaudeau, 2012: The impact of heat islands on mortality in Paris during the August 2003 heat wave. *Environ. Health Perspect.*, **120**, 254–259, https://doi.org/10.1289/ehp.1103532.

Leal Filho, W., L. Echevarria Icaza, V. O. Emanche, and A. Quasem Al-Amin, 2017: An evidence-based review of impacts, strategies and tools to mitigate urban heat islands. *Int. J. Environ. Res. Public Health*, **14**, 1600, https://doi.org/10.3390/ijerph14121600.

Madelin, M., and V. Dupuis, 2019: Intensité et délimitation de l'îlot de chaleur urbain sur la région parisienne à partir de données participatives. *Climatologie*, **17**, 9, https://doi.org/10.1051/climat/202017009.

Mahoney, W. P., III, and J. M. O'Sullivan, 2013: Realizing the potential of vehicle-based observations. *Bull. Amer. Meteor. Soc.*, **94**, 1007–1018, https://doi.org/10.1175/BAMS-D-12-00044.1.

Meier, F., D. Fenner, T. Grassmann, B. Jänicke, M. Otto, and D. Scherer, 2015: Challenges and benefits from crowd sourced atmospheric data for urban climate research using Berlin, Germany, as testbed. *Ninth Int. Conf. Urban Climate/12th Symp. on the Urban Environment*, Toulouse, France, IAUC and Amer. Meteor. Soc., http://www.meteo.fr/icuc9/LongAbstracts/nomtm6-2-6171335_a.pdf

——, ——, ——, M. Otto, and D. Scherer, 2017: Crowdsourcing air temperature from citizen weather stations for urban climate research. *Urban Climate*, **19**, 170–191, https://doi.org/10.1016/j.uclim.2017.01.006.

Muller, C. L., L. Chapman, C. S. B. Grimmond, D. T. Young, and X. Cai, 2013: Sensors and the city: a review of urban meteorological networks. *Int. J. Climatol.*, **33**, 1585–1600, https://doi.org/10.1002/joc.3678.

——, ——, S. Johnston, C. Kidd, S. Illingworth, G. Foody, A. Overeem, and R. Leigh, 2015: Crowdsourcing for climate and atmospheric sciences: current status and future potential. *Int. J. Climatol.*, **35**, 3185–3203, https://doi.org/10.1002/joc.4210.

Napoly, A., T. Grassmann, F. Meier, and D. Fenner, 2018: Development and application of a statistically-based quality control for crowdsourced air temperature data. *Front. Earth Sci.*, **6**, 118, https://doi.org/10.3389/feart.2018.00118.

Oke, T. R., 2004: Initial guidance to obtain representative meteorological observations at urban sites. WMO Instruments and Observing Methods Rep. 81, WMO/TD-1250, 47 pp., https://library.wmo.int/doc_num.php?explnum_id=9286.

——, G. Mills, A. Christen, and J. A. Voogt, 2017: *Urban Climates.* Cambridge University Press, 548 pp.

Overeem, A., J. R. Robinson, H. Leijnse, G.-J. Steeneveld, B. P. Horn, and R. Uijlenhoet, 2013: Crowdsourcing urban air temperatures from smartphone battery temperatures. *Geophys. Res. Lett.*, **40**, 4081–4085, https://doi.org/10.1002/grl.50786.

Parsaee, M., M. M. Joybari, P. A. Mirzaei, and F. Haghighat, 2019: Urban heat island, urban climate maps and urban development policies and action plans. *Environ. Technol. Innovation*, **14**, 100341, https://doi.org/10.1016/j.eti.2019.100341.

Perkins-Kirkpatrick, S., and S. Lewis, 2020: Increasing trends in regional heatwaves. *Nat. Commun.*, **11**, 3357, https://doi.org/10.1038/s41467-020-16970-7.

Pohl, B., and Coauthors, 2015: L'Ilot de Chaleur Urbain de l'agglomération dijonnaise: Campagne instrumentale in situ et modélisation climatique régionale haute résolution. *Workshop MISTRALS "Modélisation climatique régionale intégrée,"* Toulouse, France, Météo-France, 30 pp., https://hal.archives-ouvertes.fr/hal-02159119.

R Core Team, 2019: R: A language and environment for statistical computing. R Foundation for Statistical Computing, https://www.R-project.org/.

Richard, Y., and Coauthors, 2018: How relevant are local climate zones and urban climate zones for urban climate research? Dijon (France) as a case study. *Urban Climate*, **26**, 258–274, https://doi.org/10.1016/j.uclim.2018.10.002.

——, and Coauthors, 2021: Is urban heat island intensity higher during hot spells and heat waves (Dijon, France, 2014–2019)? *Urban Climate*, **35**, 100747, https://doi.org/10.1016/j.uclim.2020.100747.

Riede, H., and Coauthors, 2019: Passenger car data – A new source of real-time weather information for nowcasting, forecasting, and road safety. *Third European Nowcasting Conf.*, Madrid, Spain, AEMET, 15 pp., https://edrop.zamg.ac.at/owncloud/index.php/s/9tiKLz9JFisqPCP/download.

Ritchie, H., and M. Roser, 2018: Urbanization. Our World in Data, https://ourworldindata.org/urbanization.

Salvati, A., H. Coch Roura, and C. Cecere, 2017: Assessing the urban heat island and its energy impact on residential buildings in Mediterranean climate: Barcelona case study. *Energy Build.*, **146**, 38–54, https://doi.org/10.1016/j.enbuild.2017.04.025.

Siems-Anderson, A., C. Walker, G. Wiener, W. Mahoney, and S. Haupt, 2019: An adaptive big data weather system for surface transportation. *Transp. Res. Interdiscip. Perspect.*, **3**, 100071, https://doi.org/10.1016/j.trip.2019.100071.

——, J. A. Lee, B. Brown, G. Wiener, and S. Linden, 2020: Impacts of assimilating observations from connected vehicles into a numerical weather prediction model. *Transp. Res. Interdiscip. Perspect.*, **8**, 100253, https://doi.org/10.1016/j.trip.2020.100253.

Stewart, I. D., 2011: A systematic review and scientific critique of methodology in modern urban heat island literature. *Int. J. Climatol.*, **31**, 200–217, https://doi.org/10.1002/joc.2141.

——, and T. R. Oke, 2012: Local climate zones for urban temperature studies. *Bull. Amer. Meteor. Soc.*, **93**, 1879–1900, https://doi.org/10.1175/BAMS-D-11-00019.1.

Tan, J., and Coauthors, 2010: The urban heat island and its impact on heat waves and human health in Shanghai. *Int. J. Biometeorol.*, **54**, 75–84, https://doi.org/10.1007/s00484-009-0256-x.

UN Department of Economic and Social Affairs, 2018: World urbanization prospects 2018. United Nations, accessed 19 June 2021, https://population.un.org/wup/DataQuery/.

Varentsov, M. I., T. E. Samsonov, P. E. Kargashin, P. A. Korosteleva, A. I. Varentsov, A. A. Perkhurova, and P. I. Konstantinov, 2020: Citizen weather stations data for monitoring applications and urban climate research: An example of Moscow megacity. *IOP Conf. Ser. Earth Environ. Sci.*, **611**, 012055, https://doi.org/10.1088/1755-1315/611/1/012055.

Venter, Z. S., O. Brousse, I. Esau, and F. Meier, 2020: Hyperlocal mapping of urban air temperature using remote sensing and crowdsourced weather data. *Remote Sens. Environ.*, **242**, 111791, https://doi.org/10.1016/j.rse.2020.111791.

Yamato, H., T. Mikami, and H. Takahashi, 2017: Impact of sea breeze penetration over urban areas on midsummer temperature distributions in the Tokyo Metropolitan area. *Int. J. Climatol.*, **37**, 5154–5169, https://doi.org/10.1002/joc.5152.

Zumwald, M., B. Knüsel, D. N. Bresch, and R. Knutti, 2021: Mapping urban temperature using crowd-sensing data and machine learning. *Urban Climate*, **35**, 100739, https://doi.org/10.1016/j.uclim.2020.100739.